ELSEVIER

Neurobiology of Aging 22 (2001) 217–226

NEUROBIOLOGY OF AGING

www.elsevier.com/locate/neuaging

Visualization of fibrillar amyloid deposits in living, transgenic *Caenorhabditis elegans* animals using the sensitive amyloid dye, X-34

Christopher D. Link[a,*], Carolyn J. Johnson[a], Virginia Fonte[a], Marie-Christine Paupard[b], David H. Hall[b], Scot Styren[c], Chester A. Mathis[d], William E. Klunk[e]

[a]*Institute for Behavioral Genetics, University of Colorado, Campus Box 447, Boulder, CO 80309, USA*
[b]*Department of Neuroscience, Albert Einstein College of Medicine, Bronx, NY 10461, USA*
[c]*Aventis Pharmaceuticals, Bridgewater, NJ 08807, USA*
[d]*Department of Radiology, PET Facility, University of Pittsburgh School of Medicine, Pittsburgh, PA 15213, USA*
[e]*Department of Psychiatry, University of Pittsburgh School of Medicine, Pittsburgh, PA 15213, USA*

Received 18 August 2000; received in revised form 6 October 2000; accepted 17 October 2000

Abstract

Transgenic *Caenorhabditis elegans* animals can be engineered to express high levels of the human beta amyloid peptide (Abeta). Histochemistry of fixed tissue from these animals reveals deposits reactive with the amyloid-specific dyes Congo Red and thioflavin S (Fay et al., *J. Neurochem* 71:1616, 1998). Here we show by immuno-electron microscopy that these animals contain intracellular immunoreactive deposits with classic amyloid fibrillar ultrastructure. These deposits can be visualized in living animals using the newly developed, intensively fluorescent, amyloid-specific dye X-34. This in vivo staining allows monitoring of amyloid deposition in individual animals over time. The specificity of this staining is demonstrated by examining transgenic animals expressing high levels of a non-fibrillar beta peptide variant, the beta single-chain dimer. These animals have deposits immunoreactive with anti-beta antibodies, but do not have X-34 deposits or deposits with a fibrillar ultrastructure. X-34 can also be used in vivo to visualize putative amyloid deposits resulting from accumulation of human transthyretin, another amyloidic protein. In vivo amyloid staining with X-34 may be a useful tool for monitoring anti-amyloidic treatments in real time or screening for genetic alterations that affect amyloid formation.

Keywords: Abeta; Amyloid; C. elegans; Transgenic; X-34; In vivo staining; Immuno-EM; Fibrillar ultrastructure; Transthyretin; 4G8; BSB

1. Introduction

Deposits of aggregated, fibrillar proteins are associated with a number of age-associated human diseases [14]. These deposits can be either predominantly extracellular (e.g. Abeta in Alzheimer's disease, transthyretin in familial amyloid polyneuropathy) or intracellular (e.g. α-synuclein in Parkinson's disease, tau in frontotemporal dementia). The relationship between these deposits and the cellular pathology observed in these diseases is unclear; numerous models have been developed to investigate whether this association is directly causal. We have employed the intensely-studied nematode worm, *Caenorhabditis elegans*, to develop one such model. Transgenic *C. elegans* animals can be engineered, using a body wall muscle-specific promoter, to express high levels of the human Abeta peptide, leading to the production of amyloid deposits and a progressive paralysis phenotype [15]. This model system has been successfully used to investigate the role of Abeta primary sequence in in vivo amyloid formation [5]. Although these animals clearly form deposits reactive with the classic amyloid dyes Congo Red and thioflavin S, the precise cellular location of these deposits has not been determined. It has also been difficult to determine the evolution and distribution of these deposits over time, given the relative insensitivity of these staining techniques (e.g. in comparison to antibody staining) and the small physical dimensions of these animals. Because these issues are directly relevant to understanding the cellular pathology observed in these transgenic animals, we have employed immuno-EM and a novel in vivo staining protocol to localize these deposits.

The association of amyloid deposits with disease has also stimulated the development of improved probes for amyloid deposits, as well as compounds to inhibit amyloid forma-

* Corresponding author. Tel.: +1-303-735-5112; fax: +1-303-492-8063.
E-mail address: linkc@colorado.edu (C.D. Link).

0197-4580/01/$ – see front matter
PII: S0197-4580(00)00237-2

Table 1
Transgenic strains used in this study

Strain	Human protein expressed	Transgenic marker	Reference
CL2006	Abeta	Rol-6	[15]
CL2008	Transthyretin	Rol-6	[15]
CL2099	None	Rol-6	[5]
CL2109	Abeta dimer	Rol-6	[5]
CL2120	Abeta	Mtl-2/GFP	[5]

tion. One such probe is X-34 [1,4-bis(3-carboxy-4-hydroxyphenylethenyl)-benzene], a recently developed, intensely fluorescent Congo Red derivative that can sensitively detect amyloid in neuritic and diffuse plaques in post-mortem AD brain tissue [23]. A nearly identical compound, termed BSB, has recently been shown to enter the brain of Tg2576 transgenic mice after repeated intraveneous injections in DMSO [21]. This compound showed labeling of amyloid plaques in ex vivo examinations of the brain by fluorescence microscopy. BSB is a simple chemical derivative of X-34, previously described by Klunk et al. [13], differing only by substitution of a bromine for a hydrogen atom. We show here that X-34, in addition to sensitively labeling amyloid deposits in the AD brain, also sensitively and specifically detects amyloid deposits in transgenic *C. elegans* animals expressing human Abeta. The natural transparency of *C. elegans*, which has allowed the use of endogenous fluorescent reporters such as Green Fluorescent Protein (GFP) in living animals [2], has also enabled us to directly investigate whether X-34 can stain amyloid in vivo. This question is of importance given the ultimate goal of developing probes which will allow diagnostic imaging of amyloid in living patients using non-invasive techniques such as PET or SPECT.

2. Experimental procedures

2.1. Transgenic strains

The construction and characterization of the transgenic nematode strains used in this work have been previously described (see Table 1). Animals were propagated at 18–20°C on NGM agar plates seeded with *E. coli* as a food source [4].

2.2. Immuno-EM

Mixed stage populations of CL2006 or CL2099 were fixed using a modification of previously described microwave fixation protocols [9,11]. Nematodes were fixed in 4% paraformaldehyde, 0.1 M sucrose, 0.05 mM $MgCl_2$ in 0.1 M HEPES pH 7.5 using a specialized microwave oven (Ted Pella) with adjustable energy levels and programmable pulse regimes. A 1–2 ml sample of fixative containing worms in a glass multi-well dish was positioned at a microwave hot spot, and the dish was bathed in 100 ml of ice. Microwave energy was set to 50% with a regime of 2 min. on, 2 min. off, repeated over a period of 10 min. (The ice loads rechilled the sample between each microwave sample so the worms never became heated above 10°C.) After aldehyde fixation, samples were washed in cold buffer and embedded in 3% agarose (Sigma type VII agarose) as a dense pellet. After overnight curing of the agarose (4°C), small blocks were cut, dehydrated in graded methanol, and embedded into LR Gold resin. Specimens were placed into gelatin capsules and cured overnight under UV in a Pella cryochamber at −2°C as previously described [8]. Thin sections were cut and collected onto nickel mesh grids, then incubated with anti-amyloid beta monoclonal antibody 4G8 (Senentec) at a concentration of 6–8 μg/ml and 10 nm gold-labeled goat anti-mouse secondary antibody (Amersham) as previously described [8]. After washing in phosphate buffer the sections were fixed in gluteraldehyde and counterstained with 2% uranyl acetate. Sections were observed with a Philips CM10 electron microscope.

2.3. Light microscopy of fixed whole mounts and sections

For immunohistochemistry of whole mounts, animals were fixed in 4% paraformaldehyde in PBS for 24 h at 4°C, rinsed, resuspended in water, then quick frozen as a slurry in liquid nitrogen. The frozen animals were then crushed under liquid nitrogen with a mortar and pestle, resulting in the breakage of almost all animals. Crushed animals were thawed and sequentially probed with anti-amyloid beta peptide monoclonal antibody 4G8 (5 μg/ml in PBS containing 1% BSA, 0.5% Triton-X 100, 0.05% sodium azide, and 1 mM EDTA) for 2 h at room temperature and then Texas Red-conjugated goat anti-mouse Ig secondary antibody (20 μg/ml in the same buffer, 2 h at room temperature). Antibody-stained animals were rinsed and incubated in 10 μM X-34 (synthesized according to the method of Styren et al.) in 40% ethanol, 10 μM Tris pH 8.0 for 5 min at room temperature, quickly rinsed in 10 mM Tris pH 7.5, then mounted for photomicroscopy and imaged using an Axioskop epifluorescence microscope.

For histochemistry of fixed sections, animals were fixed as described above, then resuspended in 1.5% Sea Plaque low melting temperature agarose at 37°C. After solidification of the agarose, small blocks (~4 × 8 × 3 mm) were cut and infiltrated with a PEG 4000 series as described by Holtham and Slepecky [10]. The final 100% PEG-infiltrated blocks were solidified by cooling on dry ice, and 10 μm sections were cut at room temperature on an American Optical microtome. Sections were transferred to silanized slides using 3% agarose blocks [6] and incubated in PBS containing 1% BSA, 0.5% Triton X-100, 0.05% sodium azide, 15U/ml rhodamine phalloidin (Molecular Probes) and 2 μM X-34 for 2 h at room temperature.

For immunohistochemistry of animals stained with X-34

while alive, animals were stained with X-34 as described below, then fixed in paraformaldehyde and permeabilized using beta-mercaptoethanol and collagenase as previously described [17]. Permeabilized animals were probed with monoclonal antibody 4G8 and secondary antibody as described above.

2.4. Staining and microscopy of living animals

Live transgenic animals were incubated in X-34 over a range of concentrations and times, and it was empirically determined that incubation in 1 mM X-34 (in 10 mM Tris pH 8.0) for two hours at room temperature gave robust and reproducible staining. X-34 uptake appeared to be passive through the mouth and anal openings. After staining, animals were subsequently returned to seeded NGM plates (6–16 h) to allow destaining via normal metabolism. Stained animals were mounted on agar pads and observed with a Zeiss Axiophot epifluorescence microscope using the "01" filter set (excitation: bandpass 365 ± 12 nm, emission: longpass 397 nm). (Note that although Styren et al. recommend excitation at 400–410 nm and an emission longpass filter of 455 nm for optimal visualization of X-34, the common filter set used here gave acceptable results.) Images were acquired using a CCD camera or 35 mm film. For 35 mm photography, animals were anesthetized by incubation in 0.1% sodium azide before mounting. Photomicrographs were digitized, and final images were fused and adjusted for brightness and contrast with Adobe Photoshop. For multiple observations of individual animals, animals were not anesthetized, and images were acquired using a high sensitivity monochrome digital camera (Intelligent Imaging Innovations). Direct digital acquisition was essential for this experiment, as the ~30 s exposure to short wave illumination required for film-based photography was toxic to the animals.

3. Results

3.1. Immuno-EM

Transgenic animals with muscle-specific expression of Abeta (strain CL2006), as well as non-expressing transgenic control animals (strain CL2099), were processed for immuno-EM using a microwave fixation protocol (see Experimental procedures). The anti-Abeta antibody used in this study, monoclonal antibody 4G8, is well-characterized and has previously been used for immunohistochemistry with these transgenic animals [5]. As shown in Fig. 1A (top panel), detection of 4G8 binding with gold-labeled secondary antibody reveals the presence of intracellular immunoreactive inclusions in the muscle cells of strain CL2006. These inclusions were not observed in the control CL2099 or wild type animals. When these inclusions were viewed at higher magnification, some could be seen to have a fibrillar ultrastructure (Fig. 1A, lower panel). Although the immuno-EM technique employed here limits high magnification resolution, these fibrils are roughly 10 nm in diameter, consistent with the morphology of beta amyloid fibrils observed in the human brain and other tissues [12,19].

We have also examined the ultrastructure of beta peptide deposits in a transgenic strain (CL2109) that expresses a putative non-amyloidic beta peptide variant, the beta peptide single chain dimer. This engineered beta peptide variant contains two head-to-tail beta 1–42 sequences joined by a linker region. Transgenic animals expressing this variant show extensive immunoreactive deposits but do not have thioflavin S deposits, suggesting that this variant is inherently non-amyloidic [5]. When processed for immuno-EM as described above, CL2109 animals also contained 4G8-binding muscle inclusions, which were often more extensive than those observed in CL2006 animals (see Fig. 1B, top panel). However, these inclusions did not show the fibrillar ultrastructure observed in animals expressing the wild type beta peptide (see Fig. 1B, bottom panel). In both strains, specific immunoreactivity was limited to body wall muscles, generally localized internal to the sarcomeres.

3.2. X-34 staining of fixed whole mounts and sections

To investigate if X-34 produced a staining pattern consistent with the distribution of amyloidic deposits revealed by immuno-EM, fixed animals were permeabilized by breakage and stained with anti-Abeta monoclonal antibody 4G8 and X-34. As shown in Fig. 2A, Abeta immunoreactivity and X-34 deposits are both localized to the longitudinal body muscle quadrants. However, there is clearly not a one-to-one correspondence between immunoreactive and dye-reactive deposits, an observation previously reported for similar experiments using monoclonal anti-Abeta antibody 4.1 and thioflavin S staining [15]. We interpret this staining pattern to indicate that only a fraction of the beta peptide has aggregated into amyloid in these animals, consistent with the immuno-EM observations.

From the whole mount immunohistochemistry described above, it is not possible to resolve whether X-34 reactive deposits are in or on body wall muscle cells. To address this issue, cross-sections of fixed CL2006 animals were stained with X-34 and rhodamine-phalloidin, a fluorescent actin probe that effectively stains muscle sarcomere fibers in *C. elegans* [7]. As shown in Fig. 2B, X-34 stains deposits (cyan) closely apposed to, and usually interior of, phalloidin-stained muscle sarcomeres (red). This distribution of X-34 deposits closely parallels that of amyloid deposits demonstrated by immuno-EM, and supports the intracellular location of the X-34 deposits.

3.3. X-34 staining in living animals

Given the optical transparency of *C. elegans*, and the sensitive amyloid staining and lipophilicity of X-34, we

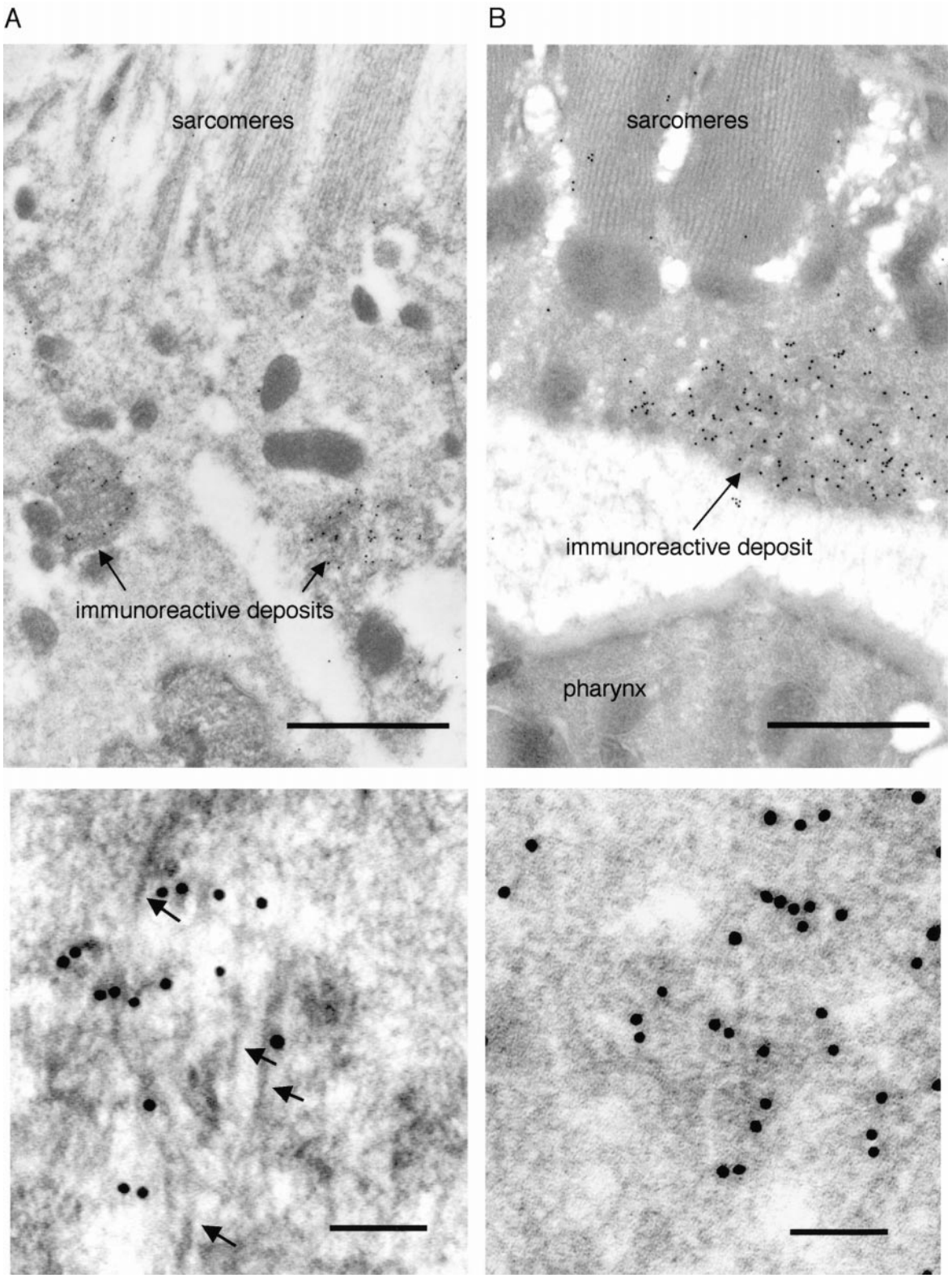

Fig. 1. Immuno-EM of transgenic *C. elegans* animals expressing wild type and variant human Abeta. A. Wild type Abeta-expressing strain CL2006, microwave fixed specimen probed with anti-Abeta monoclonal Ab 4G8 and 10 nm gold-labeled secondary antibody. Top panel: intracellular immunoreactive deposits are specifically observed in muscle cell cytoplasm. Scale bar = 1 μm. Bottom panel: Higher magnification of typical CL2006 immunoreactive deposit showing fibrillar ultrastructure (arrows). Scale bar = 100 nm B. Beta dimer variant-expressing strain CL2109, processed and imaged as in (A). Top panel: intracellular immunoreactive deposits show similar muscle-specific distribution as those observed in CL2006. Scale bar = 1 μm. Bottom panel: Higher magnification of typical CL2109 immunoreactive deposit, showing no discernible fibrillar ultrastructure. Scale bar = 100 nm.

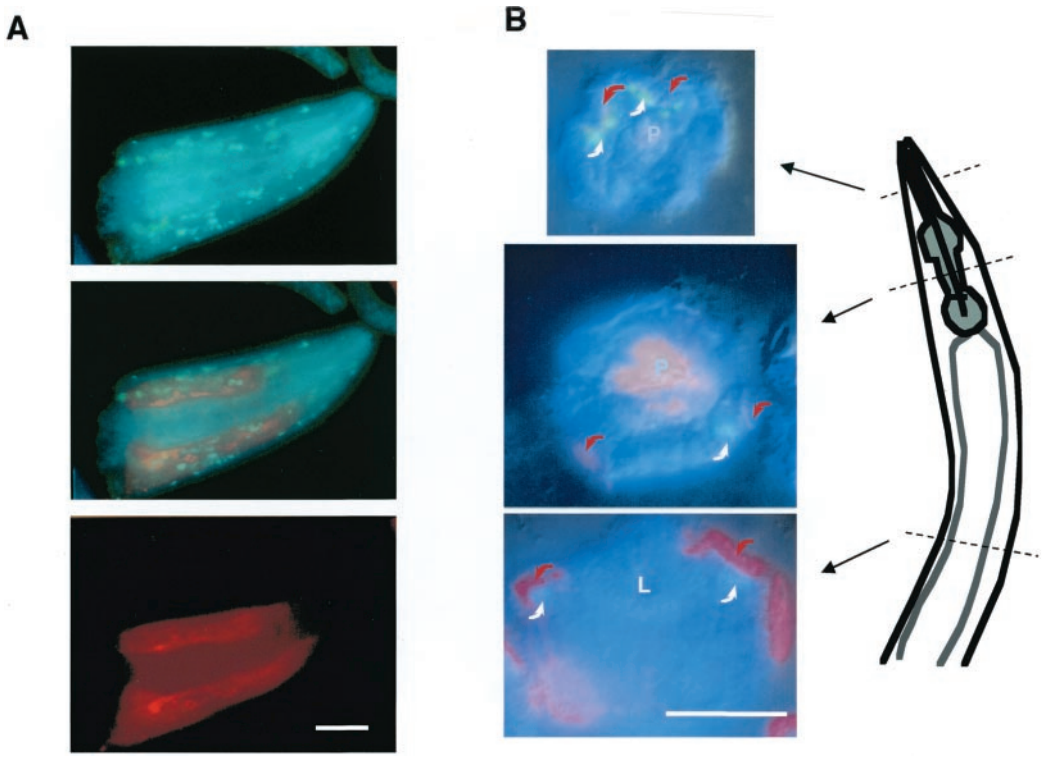

Fig. 2. X-34 staining of whole-mount and fixed sections of *C. elegans* Abeta-expressing transgenic animals. A. Anterior region of fixed, broken CL2006 animal probed with anti-Abeta peptide monoclonal antibody 4G8, Texas Red-conjugated goat anti-mouse Ig secondary antibody, and X-34. Top panel, X-34 staining visualized at short wavelength excitation; bottom panel, Abeta immunoreactivity visualized at long wavelength excitation; middle panel, digitally fused image. Scale bar = 20 μm. B. X-34 staining in fixed sections. CL2006 animals were fixed, embedded in PEG 4000, and 10 μm sections were stained with X-34 (cyan deposits, white arrows) and rhodamine-phalloidin (red arrows). Images are composites of epifluorescence and DIC photomicrographs digitally fused. Panels show representative anterior, mid-pharyngeal, and mid-body sections. *C. elegans* body wall lie in quadrants embedded in the ectoderm, surrounding the body cavity; this is most apparent in the lower panel (red arrows). Note that X-34 deposits (white arrows) are generally seen interior to the muscle sarcomeres (red arrows), consistent with the intracellular muscle distribution determined by immuno-EM. Note also that pharyngeal muscle (P, gray in the schematic drawing), sectioned in the top two panels, does not show any X-34 staining, consistent with the absence of pharyngeal muscle expression of the transgene. L = lumen of the intestine. Scale bar = 20 μm.

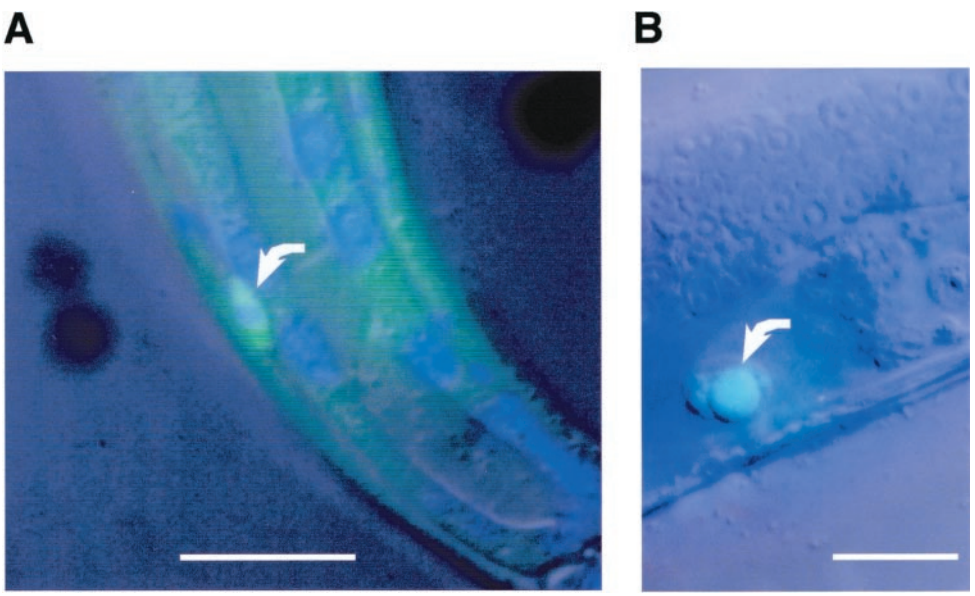

Fig. 5. Transgenic animals expressing human wild type transthyretin show specific X-34 staining of coelomocytes. A. Whole mount staining of transgenic animal expressing human transthyretin. CL2008 animals were fixed, permeabilized, and probed with polyclonal anti-transthyretin antibody and DAPI as previously described [15]. This fused DIC/epifluorescence image illustrates the specific concentration of transthyretin into a coelomocyte (arrow). (The large DAPI-stained nuclei are intestinal.) B. Specific X-34 staining in coelomocyte of living CL2008 animal. Note X-34 staining appears localized to large phagocytic vesicles in the coelomocyte. Scale bar = 20 μm.

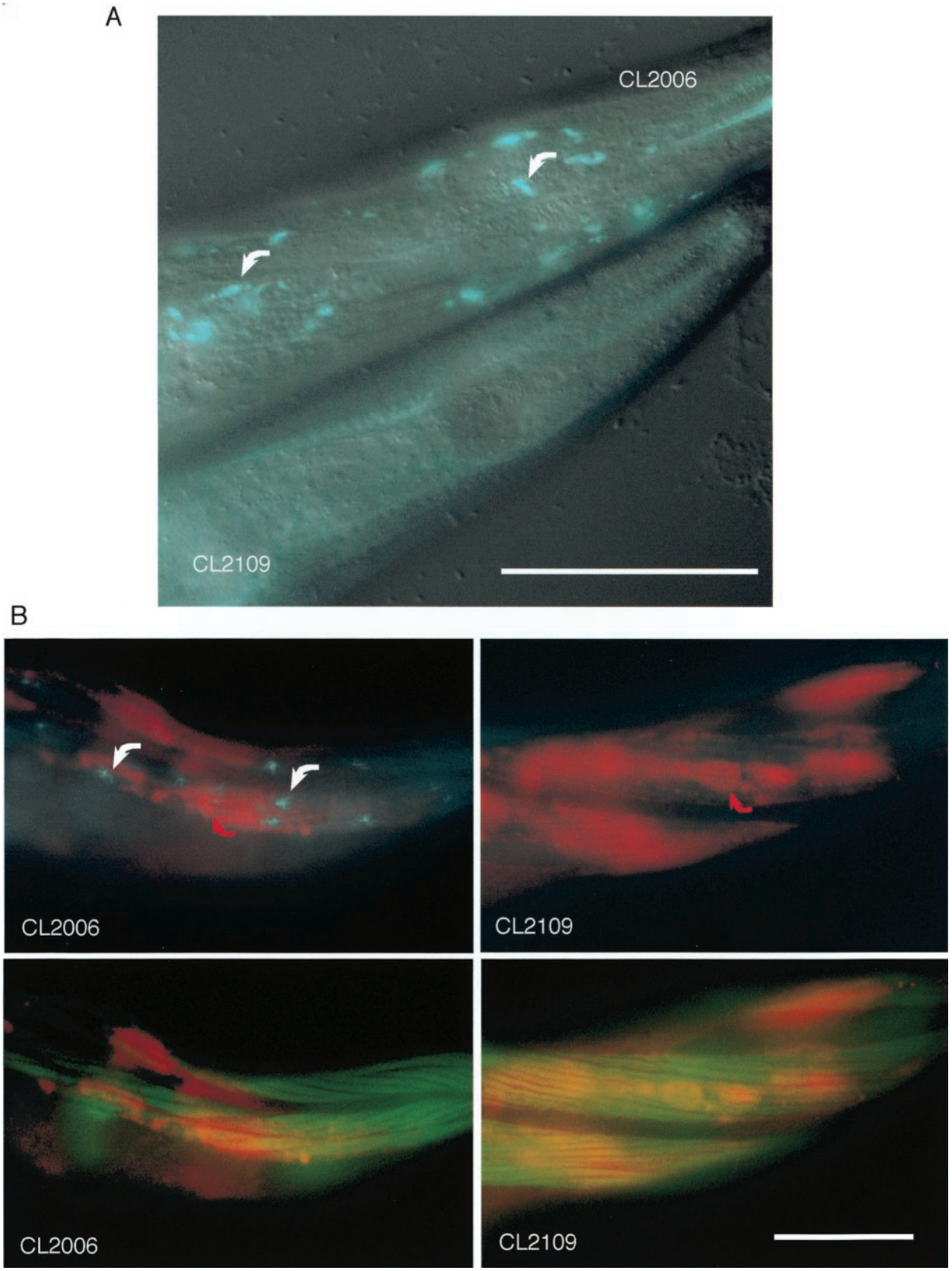
A
CL2006
CL2109
B
CL2006
CL2109
CL2006
CL2109

investigated the ability of X-34 to stain amyloid deposits in living *C. elegans* animals. As shown in Fig. 3A, deposits can readily be seen in a CL2006 animal stained and observed as a living adult, but not in a CL2109 animals similarly stained. [Deposit staining is also absent in non-expressing control transgenic animals (CL2099) or in wild type *C. elegans* (data not shown).] Note that X-34 does weakly stain the anterior buccal cavity in all animals. When live X-34 stained animals from the same populations used in Fig. 3A were fixed and probed with 4G8 and phalloidin, it was clear that although both CL2006 and CL2109 had extensive, muscle-specific immunoreactive deposits (Fig. 3B, bottom panels), X-34 deposits were only seen in the CL2006 animals expressing wild type, aggregating beta amyloid peptide (Fig. 3B, top panels).

Since X-34 incubation does not appreciably affect the growth or health of *C. elegans* animals, we investigated whether X-34 could be used to follow amyloid plaque distribution and morphology over time in individual animals. CL2120 animals were stained as larvae, digitally imaged, then returned to the culture plate. These animals were subsequently restained and re-imaged at two more time points. (CL2120 animals, which contain the same Abeta expression transgene as CL2006 [5], were chosen for this experiment because they lack the dominant Roller marker gene contained in CL2006, which causes a helically-twisted musculature that complicates repeated identification of specific amyloid deposits.) As shown in Fig. 4, this allows multiple imaging of individual amyloid plaques over time. These studies revealed that larval CL2120 animals (including animals stained shortly after hatching) contain significant numbers of amyloid deposits, which had not been previously detected using apparently less-sensitive thioflavin S staining.

3.4. X-34 staining in transgenic animals expressing human transthyretin

X-34 was also used to re-examine transgenic animals expressing human transthyretin, another potentially amyloidic protein. Previous studies have demonstrated that transgenic strain CL2008 expresses high levels of human transthyretin, which is secreted from muscles cells and distributed throughout the animal [15]. Despite this high level of transthyretin expression, these animals did not show thioflavin S-reactive deposits. When living CL2008 animals were stained with X-34, staining was observed specifically in coelomocytes, phagocytic cells that apparently take up and concentrate transthyretin from the body cavity. As shown in Fig. 5, this X-34 staining was most obvious in the large phagocytic vesicles of these coelomocytes. (Coelomocytes can be easily identified independent of staining by their morphology under DIC optics). Coelomocyte staining by X-34 was not observed in wild type or transgenic control animals (data not shown).

4. Discussion

The immuno-EM and X-34 staining results presented here demonstrate that transgenic *C. elegans* animals expressing human Abeta peptide contain intracellular amyloid deposits. The intracellular location of these deposits is somewhat surprising because the Abeta minigene construct contains a signal peptide that is apparently properly cleaved [15]. It therefore appears that although the Abeta peptide is routed to the secretory pathway, it is secreted inefficiently from (or reabsorbed efficiently into) the muscle cells that synthesize it. It is possible that the rapid aggregation of Abeta into amyloid simply precludes its secretion. However, this interpretation is inconsistent with the observation that, in animals expressing wild type Abeta, the load of immunoreactive deposits is significantly greater than those binding amyloid dyes, suggesting that at any time point much of the Abeta is not aggregated into an amyloid form. This situation is more dramatic in the Abeta single chain dimer animals, which show no evidence of amyloid formation, yet still contain only muscle-specific immunoreactive deposits. We favor the idea that Abeta is recognized as an abnormal protein, and is actively re-routed to prevent its secretion. Transgenic expression of Abeta in muscle cells leads to a strong muscle-specific induction of the small heat shock protein HSP-16 ([16], C.D.L., unpublished results),

Fig. 3. Comparison of live X-34 staining in animals expressing wild type or variant Abeta. A. Living CL2006 and CL2109 adult transgenic animals were stained in parallel with X-34 (see Experimental procedures), anesthetized and simultaneously imaged. Shown is fused DIC/epifluorescence image. The CL2006 animal (top), expressing wild type Abeta, shows clear X-34 deposits (arrows). These deposits are absent from the CL2109 animal (bottom), which expresses a non-amyloidic single chain Abeta dimer. Note that both animals show weak staining of the anterior buccal cavity (anterior is to the right). This structure is composed of sclerotized collagen and also binds thioflavin S (e.g. see Fig. 5D in [5]). Scale bar = 20 μm. B. Abeta immunoreactivity in X-34-stained CL2006 and CL2109. Animals from the same live-stained X-34 populations described in (A) were fixed, permeabilized, and probed with 4G8 and Alexa 488-conjugated phalloidin. Top left panel: CL2006 animal, fused shortwave (X-34) and longwave (4G8) epifluorescence images. Note persisting X-34 deposits (white arrows) and extensive immunoreactive material (red arrow). Both immunoreactive and X-34 deposits are closely associated with muscle sarcomeres (green), consistent with the immuno-EM observations [bottom left panel, fused FITC (phalloidin)/longwave (4G8) epifluorescence images]. Top right panel: CL2109 animals, fused shortwave (X-34) and longwave (4G8) epifluorescence images. Note complete absence of X-34 deposits despite extensive immunoreactive material (red arrow). Again, immunoreactive deposits are closely associated with muscle sarcomeres (bottom right panel). Scale bar = 20 μm. All images for this figure were acquired with a monochrome CCD camera, and are thus false color.

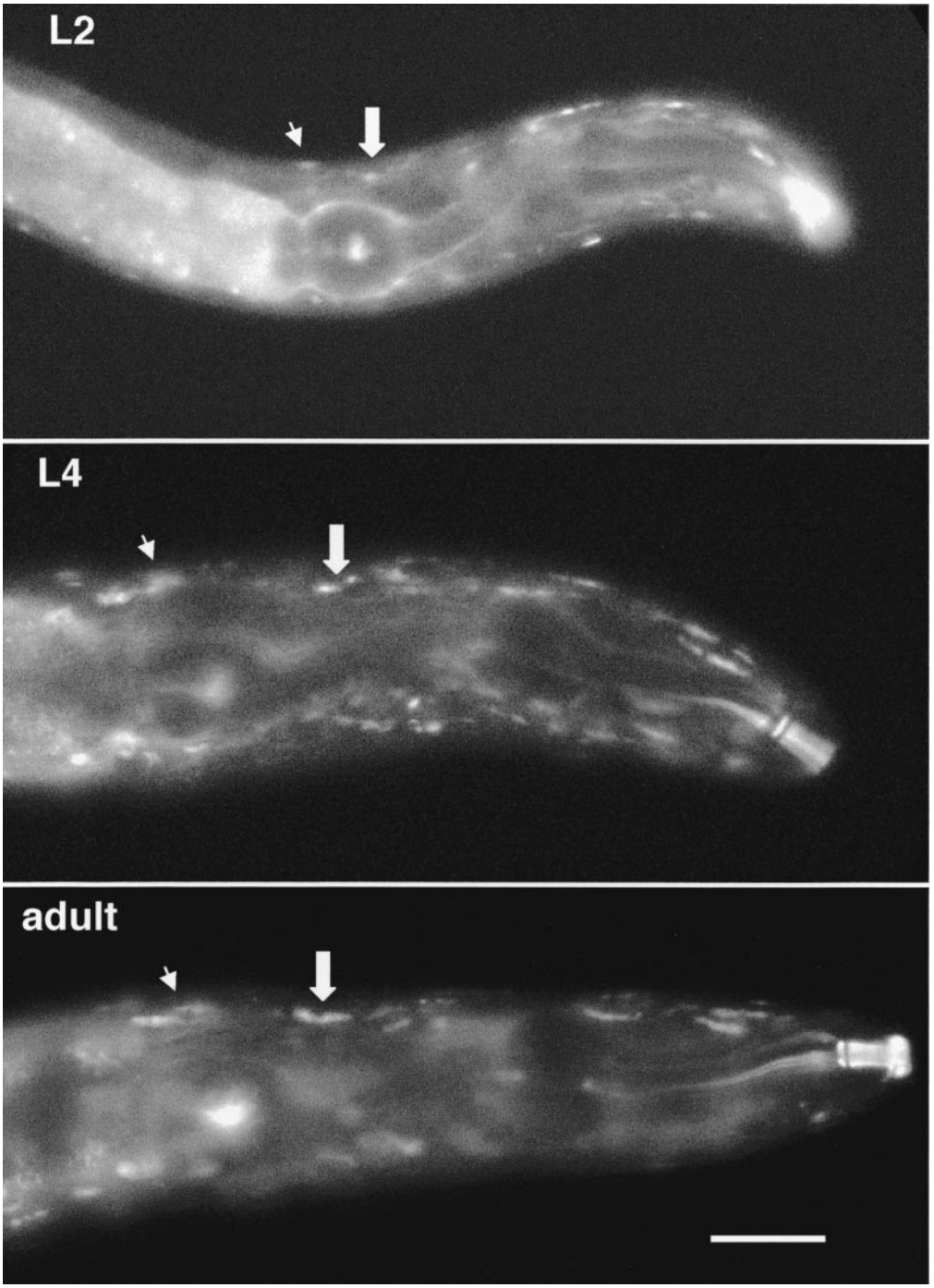

Fig. 4. Monitoring of X-34 deposits over time in an individual living transgenic animal expressing wild type Abeta. The representative animal shown in this figure was stained as a first stage larva, destained for 12 h, then imaged as a second stage larva (L2). This animal was allowed to recover for one day on a standard culture plate, similarly stained and destained, then reimaged as a fourth larval stage (L4). This schedule of recovery, restaining, and destaining was repeated to generate the final adult image. Note the two specific X-34 deposits indicated by the thin and thick arrows, which lie in a left dorsal muscle quadrant apposed to the pharyngeal bulb. These deposits appear to increase in size and signal intensity over time. Scale bar = 20 μm.

which may be a component of this proposed "active quality control." It is conceivable that a mis-folded protein response might enhance amyloid formation, given that αB crystallin (closely related to small heat shock proteins) has been reported to increase beta amyloid formation [22]. This proposed process cannot simply recognize non-native proteins, as human transthyretin is efficiently secreted from nematode muscles without any concomitant induction of HSP16.

Since the amyloid in these transgenic animals is intracellular, does this model have any relevance to Alzheimer's disease, where the large bulk of amyloid is clearly extracellular? There are a number of lines of evidence suggesting

that aggregated intracellular Abeta can accumulate in mammalian cells and play a pathological role. Cultured NT2N neurons have been shown to contain an insoluble pool of Abeta that can be recovered by formic acid extraction [20], and exposure of PC12 cells to exogenous Abeta 1–42 leads to the accumulation of an insoluble pool of newly synthesized Abeta [24]. Recent studies have also detected intracellular Abeta in hippocampal neurons of AD brains [3]. Perhaps most directly relevant to the model system described here, intracellular beta amyloid has been reported in muscle fibers from Inclusion Body Myositis patients [1]. We therefore believe that this model is relevant to amyloid disease, and that the availability of sensitive amyloid probes such as X-34, used in conjunction with confocal microscopy, will lead to the further identification of intracellular amyloid in a variety of cell types.

The intensely fluorescent nature of X-34 has allowed the identification of amyloid in Alzheimer's disease brain sections that could not be visualized with thioflavin S [23]. Similarly, X-34 staining in the *C. elegans* transgenic animals has enabled us to see previously unrecognized amyloid deposits. Because thioflavin-S and X-34 both compete for binding to the Congo red/Chrysamine-G site of amyloid fibrils (W. E. K., unpublished results), the enhanced sensitivity of X-34 is likely due to its enhanced binding affinity to this site and increased fluorescence quantum yield. We have now established that transgenic animals have significant numbers of amyloid deposits early in larval development (i.e. $<$2 days after initiation of embryogenesis), and that some animals have amyloid deposits at hatching ($\sim$12 h after likely initiation of Abeta synthesis). Repeated observation of individual X-34–stained animals indicates that the increase in amyloid load occurring from mid-larval to adult stages results from the increase in deposit size more than the appearance of new deposits, a result relevant to the design of studies using this model system to assay compounds with anti-amyloidic potential. The sensitivity of X-34 has also revealed that transgenic animals expressing human transthyretin contain amyloidic deposits specifically in large vesicles of the coelomocytes, 6 phagocytic cells known to concentrate extracellular protein from the body cavity. Although the scavenging properties of *C. elegans* coelomocytes have not been well characterized, we speculate that the apparent amyloidic form of transthyretin in these cells results from the concentration of extracellular transthyretin into acidic phagocytic vesicles that may promote beta-sheet fibril formation detectable by X-34.

Compounds that bind amyloid may potentially be able to inhibit amyloid formation, and possibly block amyloid toxicity. This property has been reported for Congo Red [18]. We have examined transgenic *C. elegans* animals propagated throughout life on media containing X-34 (1 mM) for inhibition of amyloid formation or the progressive paralysis associated with Abeta expression, but have not observed any reduction in these phenotypes, despite robust staining of the amyloid deposits themselves (C.J.J. and C.D.L., unpublished observations). This result suggests that X-34 may not be able to competitively inhibit amyloid formation, at least at the intracellular levels attainable in this model system. We also note that in this transgenic model, Abeta expression is restricted to muscle cells, and thus may not directly reflect the kinetics of amyloid formation in neuronal tissue.

Our results directly demonstrate that X-34 specifically binds amyloid in living tissue, an essential prerequisite for the development of probes for in vivo detection of amyloid in human patients. As a basic research tool, X-34 can also potentially be used in *C. elegans*, or any other transparent model organism, for the unbiased detection of novel amyloidic mutations through forward genetic screens.

Acknowledgments

The authors would like to thank Christine Martin for media preparation, and Moira Breen, Gaetan Borgonie, Gautam Kao, Raj Patel and Bill Wadsworth for help with preliminary electron microscopy studies. We would also like to thank members of the T. E. Johnson lab for helpful feedback during the course of this work. Some of the work presented here was performed at the Center for *C. elegans* Anatomy (D.H.H. and M.C.P.), supported by NIH-NCRR grant 12596. This work was also supported by NIA grant AG12423 (to C.D.L.) and by grants from the Alzheimer's Association (IIRG-95-076) and Aventis Pharmaceuticals, Inc. (to W.E.K.).

References

[1] Askanas, V., Engel, W. K., Alvarez, R. B. 1992. Light and electron microscopic localization of beta-amyloid protein in muscle biopsies of patients with inclusion-body myositis. *Am J Pathol* 141:31–6.

[2] Chalfie, M., Tu, Y., Euskirchen, G., Ward, W. W., Prasher, D. C. 1994. Green fluorescent protein as a marker for gene expression. *Science* 263:802–5.

[3] D'Andrea, M. R., Nagele, R. G., Wang, H.-Y., Plata-Salaman, C. R., Peterson, P. A. et al. 1999. Origin of amyloid plaque: new perspectives from immunohistochemical studies of Alzheimer's disease brains. *Soc. Neurosci. Abstr.* 1999 25:298.

[4] Epstein, H. F. & Shakes, D.C, eds. 1995. *Caenorhabditis elegans: modern biological analysis of an organism.* Methods in Cell Biology, Academic Press, New York, New York.

[5] Fay, D. S., Fluet, A., Johnson, C. J., Link, C. D. 1998. *In vivo* aggregation of beta-amyloid peptide variants. *J Neurochem* 71:1616–25.

[6] Gao, K. X., Godkin, J. D. 1991. A new method for transfer of polyethylene glycol-embedded tissue sections to silanated slides for immunocytochemistry. *J Histochem Cytochem* 39:537–40.

[7] Goetinck, S., Waterston, R. H. 1994. The *Caenorhabditis elegans* UNC-87 protein is essential for maintenance, but not assembly, of bodywall muscle. J *Cell Biol* 127:71–8.

[8] Hall, D. H. 1995. Electron microscopy and three-dimensional image reconstruction. *Methods Cell Biol* 48:395–436.

[9] Hall, D. H., Winfrey, V. P., Blaeuer, G., Hoffman, L. H., Furuta, T. et al. 1999. Ultrastructural features of the adult hermaphrodite gonad of *Caenorhabditis elegans*: relations between the germ line and soma. *Dev Biol* 212:101–23.

[10] Holtham, K. A., Slepecky, N. B. 1995. A simplified method for obtaining 0.5-microns sections of small tissue specimens embedded in PEG. J *Histochem Cytochem* 43:637–43.

[11] Jones, J. T., Gwynn, I. A. 1991. A method for rapid fixation and dehydration of nematode tissue for transmission electron microscopy. *J Microscopy* 164:43–51.

[12] Kawarabayashi, T., Shoji, M., Sato, M., Sasaki, A., Ho, L., Eckman CB, Prada C. M., Younkin S. G., Kobayashi T., Tada N., Matsubara E., Iizuka T., Harigaya Y., Kasai K., Hirai S. 1996. Accumulation of beta-amyloid fibrils in pancreas of transgenic mice. *Neurobiol Aging* 17:215–22.

[13] Klunk, W. E., Hamilton, R. L., Styren, S. D., Styren, G., Debnath, M. L. et al. 1997. Staining of AD and Tg2576 mouse brain with X-34, a highly fluorescent derivative of Chrisamine G and a potential in vivo probe for beta-sheet fibrils. *Soc. Neurosci. Abstr.* 1997 23:1638.

[14] Lansbury, P. T., Jr. 1999. Evolution of amyloid: what normal protein folding may tell us about fibrillogenesis and disease. *Proc Natl Acad Sci U S A* 96:3342–4.

[15] Link, C. D. 1995. Expression of human beta-amyloid peptide in transgenic *Caenorhabditis elegans. Proc Natl Acad Sci USA* 92:9368–72.

[16] Link, C. D., Cypser, J. R., Johnson, C. J., Johnson, T. E. 1999. Direct observation of stress response in *Caenorhabditis elegans* using a reporter transgene. *Cell Stress Chaperones* 4:235–42.

[17] Link, C. D., Silverman, M. A., Breen, M., Watt, K. E., Dames, S. A. 1992. Characterization of *Caenorhabditis elegans* lectin-binding mutants. *Genetics* 131:867–81.

[18] Lorenzo, A., Yankner, B. A. 1994. Beta-amyloid neurotoxicity requires fibril formation and is inhibited by congo red. *Proc Natl Acad Sci USA* 91:12243–7.

[19] Merz, P. A., Wisniewski, H. M., Somerville, R. A., Bobin, S. A., Masters, C. L., Iqbal, K. 1983. Ultrastructural morphology of amyloid fibrils from neuritic and amyloid plaques. *Acta Neuropathol (Berl)* 60:113–24.

[20] Skovronsky, D. M., Doms, R. W., Lee, V. M. 1998. Detection of a novel intraneuronal pool of insoluble amyloid beta protein that accumulates with time in culture. *J Cell Biol* 141:1031–9.

[21] Skovronsky, D. M., Zhang, B., Kung, M. P., Kung, H. F., Trojanowski, J. Q., Lee, V. M. 2000. *In vivo* detection of amyloid plaques in a mouse model of Alzheimer's disease. *Proc Natl Acad Sci USA* 97:7609–14.

[22] Stege, G. J., Renkawek, K., Overkamp, P. S., Verschuure, P., van Rijk, A. F. et al. 1999. The molecular chaperone alphaB-crystallin enhances amyloid beta neurotoxicity. *Biochem Biophys Res Commun* 262:152–6.

[23] Styren, S. D., Hamilton, R. L., Styren, G. C., Klunk, W. E. 2000. X-34, a fluorescent derivative of Congo Red: a novel histochemical stain for Alzheimer's disease pathology. *J. Histochem. Cytochem.* 48:1223–1232.

[24] Yang, A. J., Chandswangbhuvana, D., Shu, T., Henschen, A., Glabe, C. G. 1999. Intracellular accumulation of insoluble, newly synthesized abeta n-42 in amyloid precursor protein-transfected cells that have been treated with Abeta 1–42. *J Biol Chem* 274:20650–6.